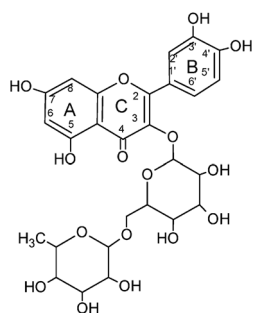


We have presented the Graphical Abstract text and image for your article below. This brief summary of your work will appear in the contents pages of the issue in which your article appears.



### Interactions of rutin with the oxidovanadium(IV) cation. Anticancer improvement effects of glycosylated flavonoids

Helen Goitia, Patricia Quispe, Luciana G. Naso, Valeria R. Martinez, Marilyn Rey, Alberto C. Rizzi, Evelina G. Ferrer and Patricia A. M. Williams\*

This work reports the biological evaluation of the new complex  $\text{Na}_2[\text{VO}(\text{rut})(\text{OH})_2] \cdot 5\text{H}_2\text{O}$  (rut = rutin, a glycosylated flavonoid).

Please check this proof carefully. Our staff will not read it in detail after you have returned it.

Please send your corrections either as a copy of the proof PDF with electronic notes attached or as a list of corrections. **Do not edit the text within the PDF or send a revised manuscript** as we will not be able to apply your corrections. Corrections at this stage should be minor and not involve extensive changes.

**Proof corrections must be returned as a single set of corrections, approved by all co-authors. No further corrections can be made after you have submitted your proof corrections as we will publish your article online as soon as possible after they are received.**

Please ensure that:

- The spelling and format of all author names and affiliations are checked carefully. You can check how we have identified the authors' first and last names in the researcher information table on the next page. **Names will be indexed and cited as shown on the proof, so these must be correct.**
- Any funding bodies have been acknowledged appropriately and included both in the paper and in the funder information table on the next page.
- All of the editor's queries are answered.
- Any necessary attachments, such as updated images or ESI files, are provided.

Translation errors can occur during conversion to typesetting systems so you need to read the whole proof. In particular please check tables, equations, numerical data, figures and graphics, and references carefully.

Please return your **final** corrections, where possible within **48 hours** of receipt, by e-mail to: njc@rsc.org. If you require more time, please notify us by email.

## Funding information

Providing accurate funding information will enable us to help you comply with your funders' reporting mandates. Clear acknowledgement of funder support is an important consideration in funding evaluation and can increase your chances of securing funding in the future.

We work closely with Crossref to make your research discoverable through the Funding Data search tool (<http://search.crossref.org/funding>). Funding Data provides a reliable way to track the impact of the work that funders support. Accurate funder information will also help us (i) identify articles that are mandated to be deposited in **PubMed Central (PMC)** and deposit these on your behalf, and (ii) identify articles funded as part of the **CHORUS** initiative and display the Accepted Manuscript on our web site after an embargo period of 12 months.

Further information can be found on our webpage (<http://rsc.li/funding-info>).

### What we do with funding information

We have combined the information you gave us on submission with the information in your acknowledgements. This will help ensure the funding information is as complete as possible and matches funders listed in the Crossref Funder Registry.

If a funding organisation you included in your acknowledgements or on submission of your article is not currently listed in the registry it will not appear in the table on this page. We can only deposit data if funders are already listed in the Crossref Funder Registry, but we will pass all funding information on to Crossref so that additional funders can be included in future.

### Please check your funding information

The table below contains the information we will share with Crossref so that your article can be found *via* the Funding Data search tool. **Please check that the funder names and grant numbers in the table are correct and indicate if any changes are necessary to the Acknowledgements text.**

Funder name	Funder's main country of origin	Funder ID (for RSC use only)	Award/grant number
Universidad Nacional de La Plata	Argentina	501100003947	X/736
Consejo Nacional de Investigaciones Científicas y Técnicas	Argentina	501100002923	0611-0550
Universidad Nacional del Litoral	Argentina	501100005746	CAI+D 2016-50420150100070LI
Agencia Nacional de Promoción Científica y Tecnológica	Argentina	501100003074	PICT 2016-1814, 2017-2186

Q1

## Researcher information

Please check that the researcher information in the table below is correct, including the spelling and formatting of all author names, and that the authors' first, middle and last names have been correctly identified. **Names will be indexed and cited as shown on the proof, so these must be correct.**

If any authors have ORCID or ResearcherID details that are not listed below, please provide these with your proof corrections. Please ensure that the ORCID and ResearcherID details listed below have been assigned to the correct author. Authors should have their own unique ORCID iD and should not use another researcher's, as errors will delay publication.

Please also update your account on our online [manuscript submission system](#) to add your ORCID details, which will then be automatically included in all future submissions. See [here](#) for step-by-step instructions and more information on author identifiers.

First (given) and middle name(s)	Last (family) name(s)	ResearcherID	ORCID iD
Helen	Goitia		
Patricia	Quispe		
Luciana G.	Naso		
Valeria R.	Martinez		
Marilyn	Rey		
Alberto C.	Rizzi		
Evelina G.	Ferrer		0000-0002-6343-5170

Patricia A. M.	Williams		0000-0002-1549-5873
----------------	----------	--	---------------------

## Queries for the attention of the authors

Journal: **NJC**





Paper: **c9nj01039d**

Title: **Interactions of rutin with the oxidovanadium(IV) cation. Anticancer improvement effects of glycosylated flavonoids**

For your information: You can cite this article before you receive notification of the page numbers by using the following format: (authors), New J. Chem., (year), DOI: 10.1039/c9nj01039d.

Editor's queries are marked on your proof like this **Q1**, **Q2**, etc. and for your convenience line numbers are indicated like this 5, 10, 15, ...

Please ensure that all queries are answered when returning your proof corrections so that publication of your article is not delayed.

Query reference	Query	Remarks
Q1	Funder details have been incorporated in the funder table using information provided in the article text. Please check that the funder information in the table is correct.	
Q2	Please confirm that the spelling and format of all author names is correct. Names will be indexed and cited as shown on the proof, so these must be correct. No late corrections can be made.	
Q3	Please check that the inserted Graphical Abstract image and text are suitable. If you provide replacement text, please ensure that it is no longer than 250 characters (including spaces).	
Q4	The sentence beginning "Moreover, it has been reported..." has been altered for clarity. Please check that the meaning is correct.	

# Interactions of rutin with the oxidovanadium(IV) cation. Anticancer improvement effects of glycosylated flavonoids†

Helen Goitia,<sup>a</sup> Patricia Quispe,<sup>a</sup> Luciana G. Naso,<sup>a</sup> Valeria R. Martínez,<sup>a</sup> Marilyn Rey,<sup>b</sup> Alberto C. Rizzi,<sup>b</sup> Evelina G. Ferrer<sup>ib</sup> <sup>a</sup> and Patricia A. M. Williams<sup>ib</sup> <sup>\*a</sup>

This work reports the biological evaluation of the new complex  $\text{Na}_2[\text{VO}(\text{rut})(\text{OH})_2] \cdot 5\text{H}_2\text{O}$  (rut = rutin, a glycosylated flavonoid). The complex was different in its coordination mode (catechol-like) from those previously reported,  $[\text{VO}(\text{rutin})(\text{H}_2\text{O})_2]_2(\text{SO}_4) \cdot 4\text{H}_2\text{O}$  and  $[\text{VO}(\text{rut})_2] \cdot 4\text{H}_2\text{O}$  (acetylacetonate-like coordination). Due to the coordination mode, the complex only improved the antioxidant activity of the ligand against superoxide and hydroxyl radicals. The results show that while both 100  $\mu\text{M}$  rutin and  $\text{V}(\text{IV})\text{O}$  did not exhibit cytotoxic activity on A549 cells, the complex selectively improved the anticancer effect ( $\text{IC}_{50} = 95 \mu\text{M}$ ), cellular reactive oxygen species (ROS) generation and depletion of the non-enzymatic antioxidant glutathione (GSH), producing oxidized glutathione (GSSG), and it did not affect the viability of the normal embryonic lung cell line (MRC-5) (up to 100  $\mu\text{M}$ ). All these data, and given the reversion of the cell killing effect of the complex upon treatment with the antioxidant agent *N*-acetyl-L-cysteine (NAC), suggested an oxidative stress mechanism. Rutin and  $\text{VO}(\text{rut})$  can spontaneously bind bovine serum albumin (BSA) and they can be stored and transported by the protein.

Received 26th February 2019,  
Accepted 19th June 2019

DOI: 10.1039/c9nj01039d

rs.c.li/njc

## 1. Introduction

Polyphenolic flavonoids are a group of natural substances with antioxidant activity. The glycoside flavonoid rutin (quercetin-3-*O*-rutinose, disaccharides: rhamnose and glucose, Fig. 1) is usually found in black tea, buckwheat and apple peel. Rutin has been investigated for its antioxidant, anti-inflammatory, anti-tumor, anti-thrombotic, cardio-protective and antibacterial activity<sup>1,2</sup> and was used as a multifunctional agent to decrease

cell adhesion and migration of human lung and colon cancer cells and to inhibit cell proliferation. All these results showed that rutin can be one of the major effective ingredients in the therapeutic treatment of cancer diseases.<sup>3</sup> In addition, due to the different coordination sites in its chemical structure it can form coordination complexes with transition metal ions ( $\text{Cu}(\text{II})$ ,  $\text{Fe}(\text{II})$ ,  $\text{Al}(\text{III})$ , and  $\text{Zn}(\text{II})$ )<sup>4,5</sup> and it has been demonstrated that its antioxidant activity was enhanced by complexation.

<sup>a</sup> Centro de Química Inorgánica (CEQUINOR-CONICET-CICPBA-UNLP), Bv. 120 No. 1465, La Plata, Argentina. E-mail: williams@quimica.unlp.edu.ar

<sup>b</sup> Departamento de Física, Facultad de Bioquímica y Ciencias Biológicas, Universidad Nacional del Litoral, 3000 Santa Fe, Argentina

† Electronic supplementary information (ESI) available: Fig. S1. Experimental powder EPR spectrum of the  $\text{Na}_2[\text{VO}(\text{rut})(\text{OH})_2] \cdot 5\text{H}_2\text{O}$  complex obtained at 120 K (black) together with the simulation (gray). Microwave frequency 9.4516 GHz. EPR parameters obtained by simulation:  $g_1 = 1.9869$ ,  $g_2 = 1.9763$ ,  $g_3 = 1.9477$ ;  $A_1 = 28.7 \times 10^{-4} \text{ cm}^{-1}$ ,  $A_2 = 51.7 \times 10^{-4} \text{ cm}^{-1}$ ;  $A_3 = 158.9 \times 10^{-4} \text{ cm}^{-1}$ . Fig. S2. (A) Spectra of rutin ( $4 \times 10^{-5} \text{ M}$ ), aqueous solutions, at different pH values. (B) Spectra of aqueous solutions of  $5 \times 10^{-5} \text{ M}$  rutin and  $2.5 \times 10^{-5} \text{ M}$   $\text{VOCl}_2$  at different pH values. (C) UV-vis spectra of rutin ( $8 \times 10^{-3} \text{ M}$ ) in DMSO with the addition of aqueous solutions of  $\text{VOCl}_2$  in ligand-to-metal ratios (L/M) from 10.0 to 0.7 (pH 7); nitrogen atmosphere. Inset: Spectrophotometric determination of the  $\text{VO}(\text{rut})$  complex stoichiometry at 820 nm. Fig. S3. Frozen EPR spectra of a DMSO solution of the  $\text{Na}_2[\text{VO}(\text{rut})(\text{OH})_2] \cdot 5\text{H}_2\text{O}$  complex (black) together with the simulation (gray). Microwave frequency 9.46546 GHz. EPR parameters obtained by simulation:  $g_1 = 1.9873$ ,  $g_2 = 1.9780$ ,  $g_3 = 1.9510$ ;  $A_1 = 26.0 \times 10^{-4} \text{ cm}^{-1}$ ,  $A_2 = 52.0 \times 10^{-4} \text{ cm}^{-1}$ ,  $A_3 = 157.7 \times 10^{-4} \text{ cm}^{-1}$ . Fig. S4. Frozen EPR spectra of a DMSO solution of  $\text{Na}_2[\text{VO}(\text{rut})(\text{OH})_2] \cdot 5\text{H}_2\text{O}$  recorded at 120 K as a function of time. Fig. S5. Effects of rutin, oxidovanadium(IV) cations and  $\text{VO}(\text{rut})$  on: (A) the reduction of nitroblue tetrazolium by the generated superoxide radical (phenazine methosulfate and reduced nicotinamide adenine dinucleotide system). (B) Peroxyl radicals generated by the thermal decomposition of AAPH (2,2-azobis(2-amidinopropane)dihydrochloride); the lag phase is the delay of the consumption of the spectrometric probe, pyranine, calculated as the time due to the consumption of peroxyl radicals by the added compounds, before the consumption of pyranine started. (C) Extent of deoxyribose degradation by hydroxyl radicals, measured with the thiobarbituric acid method. (D) Reduction of the concentration of 1,1-diphenyl-2-picrylhydrazyl radicals. The values are expressed as the mean  $\pm$  the standard error of at least three independent experiments. Fig. S6. Fluorescence emission spectra of BSA (6  $\mu\text{M}$ ) with successive addition of rutin (A) and  $\text{VO}(\text{rut})$  (B) at different concentrations (0, 5, 10, 20, 30, 40, 50, 75, and 100  $\mu\text{M}$ ). Fig. S7. Plots of  $F_0/F$  vs.  $[\text{Q}]$  for BSA with rutin and  $\text{VO}(\text{rut})$  at different temperatures ((●), 298 K; (▲), 303 K; (■), 310 K),  $\lambda_{\text{ex}} = 280 \text{ nm}$ . Table S1. Assignment of the main bands of the infrared spectra of rutin and the oxidovanadium(IV) complex  $\text{VO}(\text{rut})$  (band positions in  $\text{cm}^{-1}$ ). See DOI: 10.1039/c9nj01039d

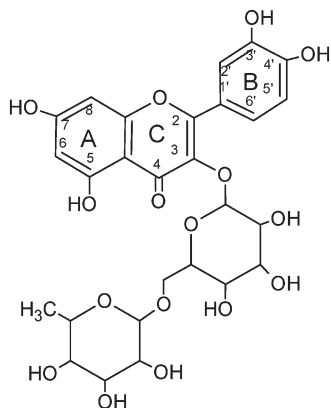


Fig. 1 Structure of rutin.

Furthermore, the anticancer activity of metal complexes is considered as one of their most important potential applications. After the discovery of cisplatin and carboplatin as potential chemotherapeutic agents, the interest in developing non-platinum metal complexes as a drug has stimulated increased research. Vanadium coordination compounds exhibited different biological effects like diabetes and lipid profile regulation, cancer regulation and apoptosis.<sup>6</sup> Hence, these kinds of complexes are suitable candidates for cancer treatment.

In previous papers we have demonstrated a structure–activity relationship on the antioxidant power of  $V(IV)O$ –flavonoid complexes. A better improvement of the antioxidant behavior of flavonoids upon complexation was found for those complexes in which the coordination sites are the carbonyl and one deprotonated OH group forming six or five membered rings, with maltol-type or acetylacetonate-type structures, respectively. In these systems the phenoxyl radicals generated by electron donation to free radicals were stabilized by the  $\pi$  electronic resonance between the  $V=O$  cation and rings A and C of the flavonoids. On the other hand, in the glycosylated derivatives the  $C=O$  group did not coordinate to the metal center and a lower improvement of the antioxidant properties of the flavonoids was determined.<sup>7</sup>

Conversely, in the A549 human cancer cell line, a better improvement of the anticancer effect and cellular ROS generation upon complexation was found for the oxidovanadium(IV) complexes with glycosylated flavonoids.<sup>8,9</sup> To confirm that this effect is due to the presence of glycosidic bonds in the flavonoid structure we have selected herein the  $V(IV)O$  complex with the glycosylated flavonoid rutin. We report the synthesis and characterization of the oxidovanadium(IV)–rutin complex  $Na_2[VO(rut)(OH)_2] \cdot 5H_2O$  and the evaluation of its antioxidant and biological properties in lung human cancer cells. Two complexes of rutin with the oxidovanadium(IV) ( $V(IV)O$ ) cation have recently been prepared and they displayed acetylacetonate-type coordination (O(4), O(5)).<sup>10,11</sup> Attempts to obtain the same complexes gave a solid complex in which rutin chelates to the metal center through a catechol-like environment (O(3'), O(4')). A similar rutin/ $V(IV)O$  complex with a

catechol-type environment has been previously prepared in the solution phase and characterized by EPR spectroscopy.<sup>12</sup> The new complex was studied using different spectroscopic techniques (FTIR, UV-vis, and EPR), TGA-DTA and elemental analyses. The flavonoid rutin displayed higher antioxidant activities than the complex against DPPH<sup>•</sup> and peroxy radicals and lower scavenging power against hydroxyl and superoxide radicals. The complex exhibited a better cytotoxic effect than rutin (tested in the human lung A549 cancer cell line) *via* an oxidative stress mechanism, without affecting the normal embryonic lung cell line (MRC-5). The ligand and complex could be carried in the bloodstream by albumin.

## 2. Experimental section

### 2.1. Materials

All chemicals were analytical grade and used without further purification. Rutin (Nanjing Zelang Medical Technology Co., Ltd) and oxidovanadium(IV) chloride (50% aqueous solution, Carlo Erba) were used as supplied. Corning or Falcon provided tissue culture materials. Dulbecco's modified Eagle's medium (DMEM) was purchased from Gibco (Gaithersburg, MD, USA); Tryple™ and fetal bovine serum (FBS) were from GibcoBRL (Life Technologies, Germany).

### 2.2. Instrumentation and methods

Elemental analysis for carbon and hydrogen was performed using a Carlo Erba EA1108 analyzer. Sodium determination was performed using a ROSS<sup>®</sup> sodium ion selective electrode (Thermo Scientific 8611BNWP). The vanadium content was determined by the tungstophosphovanadic method.<sup>13</sup> Thermogravimetric analysis (TGA) was performed with a Shimadzu system (model TG-50), working in an oxygen flow of 50 mL  $min^{-1}$  and at a heating rate of 10 °C  $min^{-1}$ . Sample quantities ranged between 10 and 20 mg. UV-vis spectra were recorded on a Shimadzu 2600/2700 spectrophotometer. Infrared spectra were measured using the KBr pellet technique with a Bruker IFS 66 FTIR spectrophotometer from 4000 to 400  $cm^{-1}$ . X-band CW-EPR spectra of a powdered sample were obtained at room (300 K) and low (120 K) temperatures on a Bruker EMX-Plus spectrometer, equipped with a rectangular cavity with 100 kHz field modulation. X-band EPR spectra of frozen solutions were recorded at 120 K, in DMSO. EPR spectra were simulated with the EasySpin toolbox based on MATLAB.<sup>14</sup> Fluorescence spectra were obtained with a Shimadzu RF-6000 spectrophotometer equipped with a pulsed xenon lamp. The molar conductance of the complex was measured using a Conductivity TDS Probe – 850084, Sper Scientific Direct, using 10<sup>-3</sup> M aqueous solutions.

### 2.3. Synthesis of $Na_2[VO(rutin)(OH)_2] \cdot 5H_2O$

Rutin (1 mmol) was dissolved completely in water (20 mL) by the addition of a NaOH solution (1 M) until a final pH value of 10. An aqueous solution (10 mL) of  $VOCl_2$  (0.5 mmol) was added with stirring and the pH of the solution decreased to 8.0. The final pH value of the solution was adjusted to 7.0 with the

1 addition of 1 M HCl and it was left stirring for 1 h at room  
temperature. Then, isopropyl alcohol was added drop by drop  
until a green solid precipitated. The solid was immediately  
filtered, washed several times with isopropyl alcohol and air-  
dried. Anal. calcd for  $C_{27}H_{40}O_{24}VNa_2$ : C, 38.5; H, 4.7; V, 6.0; Na,  
5.4. Exp.: C, 38.3; H, 4.6; V, 5.9; Na, 5.5. UV-vis data: (DMSO/  
 $H_2O$ ): 660 nm (sh), 820 nm. Thermal analysis (TGA) (oxygen  
atmosphere,  $50\text{ mL min}^{-1}$ ): in the first step (20–200 °C) five  
water molecules are lost (10.3%). The dehydrated product  
rendered  $Na_4V_2O_7$  (characterized by infrared spectroscopy)  
and the weight of the final residue was 13.5% (calc. 13.3%).  
The molar conductance of the complex measured in water,  $\Lambda_m$   
 $= 148\ (\Omega^{-1}\text{ cm}^2\text{ mol}^{-1})$ , suggested the formation of a 1:2  
electrolyte.<sup>15</sup> Elemental analysis and thermal studies allow us  
to postulate a L:M stoichiometry of 1:1. This result is sup-  
ported by spectral determinations (see below).

#### 2.4. Spectrophotometric titrations

In order to establish the stoichiometry of the complex a spectro-  
photometric method was applied. A DMSO solution of rutin ( $8$   
 $\times 10^{-3}\text{ M}$ ) was prepared. The absorption spectra of different  
concentration aqueous solutions of  $VOCl_2$  in ligand-to-metal  
molar ratios from 10 to 0.5 (pH 7) were measured.<sup>16</sup> A nitrogen  
atmosphere was used during the experiments to prevent oxida-  
tion processes.

#### 2.5. Antioxidant properties

The experimental conditions for the antioxidant determina-  
tions were set according to previous reports.<sup>17</sup> The superoxide  
dismutase (SOD) activity was examined indirectly using the  
nitroblue tetrazolium (NBT) assay. The indirect determination  
of the activity of rutin and the VOrut complex by their ability to  
inhibit the reduction of NBT by the superoxide anion (gener-  
ated by the phenazine methosulfate (PMS) and reduced nicotin-  
amide adenine dinucleotide (NADH) system) was performed.  
The capacity to scavenge hydroxyl radicals (generated by the  
ascorbate–iron– $H_2O_2$  system) has been determined with the  
thiobarbituric acid method by the measurement of the extent of  
deoxyribose degradation by hydroxyl radicals. The inhibition of  
peroxyl radicals was measured by generation of the radicals by  
the thermal decomposition of 2,2-azobis(2-amidinopropane)  
dihydrochloride (AAPH). The lag phase (delay of pyranine  
consumption) was calculated as the time before the consump-  
tion of pyranine started (marked reductions in absorbance).  
The antiradical activity of the compounds was also measured in  
terms of their capacity to scavenge DPPH• (1,1-diphenyl-2-  
picrylhydrazyl) radicals. Each experiment was performed in  
triplicate and at least three independent experiments were  
evaluated in each case.

#### 2.6. Biological assays

**2.6.1. Cell culture procedure.** The A549 human lung cancer  
cell line was obtained from ABAC (Argentinean Cell Bank  
Association INEVH, Pergamino, Buenos Aires, Argentina) and  
the MRC-5 normal embryonic lung cell line was purchased  
from IMBICE (Instituto Multidisciplinario de Biología Celular).

The human lung cancer line, A549, was maintained at 37 °C in a  
5% carbon dioxide atmosphere using DMEM supplemented  
with  $100\text{ U mL}^{-1}$  penicillin,  $100\ \mu\text{g mL}^{-1}$  streptomycin and 10%  
(v/v) fetal bovine serum as the culture medium. Human fetal  
lung fibroblast cell line MRC-5 was grown as a monolayer in  
DMEM supplemented with 20% fetal bovine serum. When 70–  
80% confluence was reached, cells were detached using PBS-  
EDTA (11 mM  $KH_2PO_4$ , 26 mM  $Na_2HPO_4$ , 115 mM NaCl, pH 7.4,  
1.3 mM EDTA) with 10% TrypLE™ (Gibco, Gaithersburg, MD,  
USA). Then, the cell suspension was grown in multi-well plates,  
6-well plates, 48-well plates, or 96-well plates, depending on the  
experiment.

**2.6.2. Cell viability assay.** Cell viability tests were per-  
formed using the MTT assay.<sup>18</sup> Cells were treated with com-  
pounds at different concentrations, and then they were  
assessed in three independent experiments. A549 cells were  
seeded at a density of  $2 \times 10^6$  per well cultured in 48-well plates  
and MRC-5 cells were seeded at a density of  $2 \times 10^4$  per well in  
96-well plates. After 24 h of incubation, cells were exposed to  
different concentrations of  $VOCl_2$ , rutin and VOrut (0, 2.5, 5, 10,  
25, 50, 75, and  $100\ \mu\text{M}$ ). The dissolution vehicle (DMSO) yielded  
a maximum final concentration of 0.5% in the treated well.  
After 24 h of incubation at 37 °C, a volume of 250  $\mu\text{L}$  of MTT  
solution was added to each well and was incubated for 2 h at  
37 °C until a purple-colored formazan product developed.  
Formazan was dissolved in acidified isopropanol (cancer cell  
line) or DMSO (normal cell line). The absorbance at 560 nm was  
measured by UV-vis spectroscopy. Using the same protocol as  
described above, the MTT assay was performed in the presence  
of NAC (*N*-acetylcysteine). Cells were pretreated with 5 mM of  
NAC for 30 min, followed by treatment with rutin and VOrut at  
the same concentrations used before for 24 h.

**2.6.3. Intracellular reactive oxygen species (ROS) genera-  
tion.** Intracellular reactive oxygen species (ROS) generated by  
the compounds were evaluated using 2',7'-  
dichlorodihydrofluorescein diacetate ( $H_2DCFDA$ , Merck, Darm-  
stadt, Germany) by a fluorometric quantitative assay. Briefly,  
cells were treated with  $VOCl_2$ , rutin and VOrut (0– $100\ \mu\text{M}$ ) for  
24 h. Then, the media were removed and cells were incubated  
with 250  $\mu\text{L}$   $H_2DCFDA$  ( $10\ \mu\text{M}$ ) solution for 1 h at 37 °C in the  
dark. The media were removed and the cell monolayers rinsed  
with PBS and lysated into 1 mL 0.1% Triton-X100. The cell  
extracts were then analyzed for the oxidized product DCF by  
fluorescence spectroscopy ( $\lambda_{exc}$ , 488 nm;  $\lambda_{em}$ , 525 nm). Results  
were presented as the percentage of fluorescence intensity  
relative to the control measurements  $\pm$  standard error. Results  
were corrected for the protein content, which was assessed by  
the Bradford method.<sup>19</sup> To validate that the ROS in cells were  
generated by the compounds, the same assay in the presence of  
the antioxidant NAC was performed. Cells were pretreated with  
5 mM of NAC for 30 min, followed by treatment with rutin and  
VOrut at different concentrations for 24 h.<sup>20</sup>

**2.6.4. Estimation of the cell glutathione (GSH) and ox-  
idized glutathione (GSSG) content.** The determination of the  
reduced (GSH) and oxidized glutathione (GSSG) content in  
treated A549 cells was performed by a modification of Hissin

1 and Hilf's method.<sup>21</sup> Standard curves of GSH and GSSG (0.01–  
1.0  $\mu\text{g mL}^{-1}$ ) were processed in parallel. Briefly, for GSH  
determinations 100  $\mu\text{L}$  aliquots were mixed with 1.8 mL of ice  
cold phosphate buffer ( $\text{Na}_2\text{HPO}_4$  0.1 M–EDTA 0.005 M, pH 8)  
5 and 100  $\mu\text{L}$  *o*-phthalaldehyde (OPT) (0.1% in methanol). For  
the determination of GSSG, 100  $\mu\text{L}$  aliquots were mixed with 1.8  
mL NaOH 0.1 M and OPT but previously and to avoid GSH  
oxidation the cellular extracts for GSSG determination were  
10 incubated with 0.04 M of *N*-ethyl-maleimide (NEM). The pro-  
tein content in each cellular extract was quantified using the  
Bradford method.<sup>19</sup> The fluorescence spectra were recorded at  
350 nm excitation and 420 nm emission wavelengths. The  
concentrations in  $\mu\text{g GSH/mg protein}$  were calculated from  
15 the respective calibration curves. The ratio GSH/GSSG was  
expressed as a percentage of the control for all the experimental  
conditions.

### 2.7. Bovine serum albumin interactions

20 To 4800  $\mu\text{L}$  of Tris–HCl (0.1 M, pH 7.4), 10  $\mu\text{L}$  of an aqueous  
solution of BSA at a final concentration of 6  $\mu\text{M}$  and 10  $\mu\text{L}$  of a  
DMSO solution of rutin or an aqueous solution of VOrut were  
added and left to rest for 1 h to ensure the formation of  
homogeneous solutions. The final concentrations of the com-  
pounds ranged between 5 and 100  $\mu\text{M}$ , and buffer was used for  
25 the control. The fluorescence intensity was measured on a  
luminescence spectrometer (excitation at 280 nm and emission  
at 350 nm) at 298, 303 and 310 K. For each sample, three  
independent replicates were performed.

### 2.8. Statistical analysis

30 Data are expressed as the mean  $\pm$  standard error (SE). The  
analysis of variance (one way ANOVA) was applied by the test of  
least significant difference (Fisher) to compare the means of  
multiple groups of measured data. Significance was defined as  
35  $p < 0.05$ .

## 3. Results and discussion

### 3.1. Characterization of the VOrut complex

40 **3.1.1. FTIR spectroscopy.** The assignments of the main  
bands of the infrared spectra of the ligand and the complex  
were performed based on previous studies on the flavonoid, its  
alkali metal salts,<sup>22</sup> and the Zn/rutin<sup>23</sup> and V(IV)O/rutin  
45 complexes.<sup>11</sup>

In previous reports, the FTIR spectrum of rutin showed the  
stretching vibration of the carbonyl group at 1654  $\text{cm}^{-1}$  and  
this band shifted to lower wavenumbers (1621  $\text{cm}^{-1}$  and 1627  
 $\text{cm}^{-1}$ ) upon coordination to V(IV)O and Zn(II), respectively.  
50 These shifts were indicative of the coordination of the carbonyl  
group to the metal centers, due to the decrease of both the  
bond strength and the charge density of the C=O group. In  
VOrut the C=O stretching band of rutin did not shift upon  
complexation, indicating that this group did not participate in  
55 metal bonding (Table S1, ESI<sup>†</sup>). The position of the V=O  
stretching band is another indication of the coordination mode

of the metal to the flavonoid. In the reported complexes with  
rutin this band was located at 983–972  $\text{cm}^{-1}$  in accordance with  
chelation through the C=O and C–O moieties at rings A and C,  
generating a delocalized  $\pi$  system that allows the resonance  
with the V=O bond, maintaining the double bond character  
5 between vanadium and oxygen atoms. In the present complex  
this band shifted to low frequencies 920  $\text{cm}^{-1}$  typical of  
catechol-like coordination involving *cis*-deprotonated OH  
groups at ring B. In this type of coordination the inductive  
effect of the negative charges on the aryloxy groups produces a  
10 lengthening of the V=O bond and a decrease in the vibrational  
wavenumber. The stretching band vibrations assigned to the  
aromatic ring B at 1505  $\text{cm}^{-1}$  shifted to 1485  $\text{cm}^{-1}$ , showing  
interaction of the metal center with the 3' and 4'-deprotonated  
OH groups of rutin. Bands related to CO stretching and COH  
15 bending at 1013  $\text{cm}^{-1}$  and 1296  $\text{cm}^{-1}$  diminished in their  
intensities or shifted, suggesting deprotonation and/or coordi-  
nation to the V=O cation. The FTIR data suggest that the  
favored metal coordination occurs through the *ortho*-hydroxyl  
groups in the B ring rather than the 5-hydroxypyran-4-one  
20 moiety.

**3.1.2. Powder EPR spectrum.** The powder EPR spectra  
obtained at low temperature (Fig. S1, ESI<sup>†</sup>) and at room tem-  
perature (not shown) were similar. The EPR spectrum of VOrut  
microcrystalline powder shows the typical eight line hyperfine  
25 splitting pattern of the <sup>51</sup>V nucleus ( $I = 7/2$ ), indicating absent (or  
almost negligible) magnetic interactions between paramagnetic  
V(IV)O<sup>2+</sup> ions in the solid complex, which would collapse the  
hyperfine interaction. The EPR spectrum is also indicative of the  
presence of only one mononuclear oxidovanadium(IV) species in  
30 the solid complex. The experimental spectrum could be well  
simulated assuming *g*- and *A*-matrices with nearly axial symmetry  
and the simulation gave:  $g_1 = 1.9869$ ,  $g_2 = 1.9763$ ,  $g_3 = 1.9477$ ;  $A_1 =$   
 $28.7 \times 10^{-4} \text{ cm}^{-1}$ ,  $A_2 = 51.7 \times 10^{-4} \text{ cm}^{-1}$ ;  $A_3 = 158.9 \times 10^{-4} \text{ cm}^{-1}$ .  
Considering the additivity relationship for VO-systems, regarding  
35 the magnitude of  $A_{\text{II}}$ <sup>24</sup> the nature of the equatorial ligands can be  
suggested. The hyperfine component  $A_{\text{II}}$  for different ligand  
composition has been calculated as:  $A_z = \sum n_i A_{z,i}$ ,  $n_i$  being the  
number of equatorial ligands of type  $i$  and  $A_{z,i}$  the contribution to  
the parallel hyperfine coupling from each of them. Considering  
40 the stoichiometry determined for the complex (see above), the  
contributions to the parallel hyperfine coupling constant were  
calculated taking into account two hydroxyl groups and one  
flavonoid molecule around the metal center ( $2\text{OH}^- = 2 \times 38.7$   
 $\times 10^{-4} \text{ cm}^{-1}$  and  $2\text{ArO}^-$  (catechol-like from one rutin molecule) =  
45  $38.6 \times 10^{-4} \text{ cm}^{-1}$ , =  $154.6 \times 10^{-4} \text{ cm}^{-1}$ .<sup>25</sup> For the ligands  
containing a catecholic donor set, the formation of square  
pyramidal complexes with ( $\text{O}^-$ ,  $\text{O}^-$ ) catechol-like coordination  
forming five-membered chelate rings is preferred at physiological  
pH values. The values of the hyperfine coupling constants were  
50 similar to those measured for V(IV)O–flavonoid complexes bear-  
ing catechol-like coordination such as 7,8-dihydroxyflavone, bai-  
calein, fisetin, and quercetin and, in particular, to the values  
previously obtained for the oxidovanadium(IV)–rutin system in  
solution at pH > 6.<sup>12</sup> However, in acidic pH ranges, the reported  
55 anisotropic EPR spectra recorded for a mixture of



oxidovanadium(IV) and rutin, in DMSO/water 1:1, showed acetylacetonate-like coordination ( $g_z$  1.941,  $A_z$   $174.9 \times 10^{-4} \text{ cm}^{-1}$ ). From the EPR parameters we conclude that the conformation of the complex would correspond to a binding mode of  $2(\text{OH}^-, \text{ArO}^-)$ . Hence, the simulation predicted that the observed signal originating from a vanadium chromophore is consistent with catechol-like coordination of the oxidovanadium(IV) ion, in good agreement with the FTIR spectrum.

### 3.2. Solution studies

**3.2.1. UV-vis spectroscopy.** The electronic UV-vis spectrum of rutin has previously been described.<sup>22,23,26</sup> Rutin exhibited two bands at 258 nm (band II, benzoyl ring A) and 352 nm (band I, cinnamoyl associated with the conjugated system between ring B and the carbonyl of ring C) due to  $\pi-\pi^*$  transitions. We obtained the same results in water solution but this spectral pattern changed with the pH, according to the deprotonation of the different acidic groups, depending on their  $\text{pK}_a$  values. The dissociation of rutin proceeds in the following order: 7-OH, 3'-OH, 5-OH, 4'-OH.<sup>27</sup> Then, the spectral pattern changed sequentially with the change of pH (Fig. S2A, ESI†): the band at 258 nm shifted at pH values higher than 3 to 265 nm (pH 6) and to 271 nm (pH 8) and the intensities increased while band I shifted to 390 nm (pH 6) and 399 nm (pH 8 and higher).

It is known that metal ions compete with protons for ligand binding in aqueous solution, and hence upon coordination with the acidic metal cation the  $\text{pK}_a$  constants of the ligand changed. As an example, the  $\text{pK}_a$  value of water decreases when it coordinates to Zn from 15.74 to 9.0. In particular, when the  $\text{V}(\text{IV})\text{O}$  cation coordinates to the deprotonated 3'-OH group, the  $\text{pK}_a$  value of the 4'-OH group in the *cis* position lowers and makes this position a better donor atom, generating the *ortho*-dihydroxyl (catechol) environment. The electronic spectral pattern for an aqueous mixture of  $5 \times 10^{-5} \text{ M}$  rutin and  $2.5 \times 10^{-5} \text{ M}$  oxidovanadium(IV) cations at different pH values (Fig. S2B, ESI†) showed that the band at 258 nm shifted to 265 nm (pH 4) and 275 nm (pH 5), both with similar intensities, and 270 nm (pH 8) with high intensity. Band I shifted from 350 nm to 412 nm (pH 5). At a pH value *ca.* 4, an equilibrium between two species can be observed (bands at 360 nm and 402 nm). At pH values of 5 and 8, the new band I remained at 414 nm. The red shift of band I (from 390 in rutin to 412 nm in the complex) is indicative of complex formation. It can even be seen that complex formation takes place at pH values lower than the pH of ligand deprotonation, as expected.

The visible range of the electronic spectrum displayed a band at 820 nm suggesting formation of the mono-catecholate<sup>28</sup> and resembles those of  $\text{V}(\text{IV})\text{O}$  flavonoids with catechol like coordination.<sup>7,9</sup> To determine the stoichiometry of the  $\text{VORut}$  complex in solution, a spectrophotometric titration was performed in the visible part of the electronic spectrum of a DMSO/aqueous solution of the complex, at the maximum of the  $d \rightarrow d$  transition band. The spectral patterns of different ligand-to-metal ( $8 \times 10^{-3} \text{ M}$ ) DMSO rutin solutions, pH 7, under a nitrogen atmosphere (Fig. S2C, ESI†) showed that the

band at 820 nm increased its intensity upon addition of different quantities of aqueous solutions of  $\text{V}(\text{IV})\text{O}$ . The molar ratio plot indicated the formation of a 1:1 rutin- $\text{VO}$  complex (Fig. S2C, ESI,† inset).

**3.2.2. EPR spectrum in solution.** The EPR spectrum obtained in a frozen solution at 120 K in DMSO (Fig. S3, ESI†) shows the typical eight-line pattern spectrum for  $\text{V}(\text{IV})\text{O}^{2+}$  systems. The solution experimental spectrum can be well simulated assuming *g*- and *A*-matrices with nearly axial symmetry. This signal indicated the formation of single mononuclear species after the dissolution process ( $A_z = 157.7 \times 10^{-4} \text{ cm}^{-1}$ ). The EPR parameters obtained by simulation predicted, in a similar way as for the powder EPR spectrum, that the observed signal is consistent with catechol-like coordination of the oxidovanadium(IV) ion.

**3.2.3. Stability studies.** The stability of the complex in aqueous solution was followed by UV-vis and EPR spectroscopies and conductimetric studies. The spectral changes in the electronic spectra of 6.7 mM (DMSO/ $\text{H}_2\text{O}$ ) of  $\text{VORut}$  during 60 min were negligible (data not shown). The conductimetric measurements were performed with 25 mL of an aqueous  $1 \times 10^{-3} \text{ M}$  solution of the complex, in duplicate. The values ranged from 148 to 149 ( $\Omega^{-1} \text{ cm}^2 \text{ mol}^{-1}$ ), 60 min. These values indicate that during the manipulation time for biological studies (15 min) the complex remained without decomposition. The stability of a DMSO solution of the complex was measured using EPR spectroscopy (Fig. S4, ESI†). Although the measurements were performed at 120 K (where the thermal decomposition should occur more slowly) no appreciable changes in the spectral pattern were observed, indicating that the compound remained stable for at least 60 min.

It is known that basic catechol complexes displayed different stoichiometries  $[\text{VOcat}]$ ,  $[\text{VO}(\text{cat})_2]^{2-}$  and  $[\text{V}(\text{cat})_3]^{2-}$ .<sup>29</sup> While  $[\text{VO}(\text{cat})_2]^{2-}$  showed the  $\text{V}=\text{O}$  vibrational stretching band at  $920 \text{ cm}^{-1}$ , this band is absent in the tris-catechol because the chelating ability of catechol produced the displacement of the oxidovanadium(IV) oxygen. The EPR parameters were determined as  $A_z$   $170 \times 10^{-4} \text{ cm}^{-1}$ ,  $154 \times 10^{-4} \text{ cm}^{-1}$  and  $14 \times 10^{-4} \text{ cm}^{-1}$ , respectively.<sup>30</sup> The value of  $A_z$   $157.7 \times 10^{-4} \text{ cm}^{-1}$  for  $\text{Na}_2[\text{VO}(\text{rut})(\text{OH})_2] \cdot 5\text{H}_2\text{O}$  is indicative of the presence of two rutin ligands or one rutin and two hydroxo anions (according to the additivity rule), discarding the tris-catechol complex formation, probably because of steric hindrance. Furthermore, the electronic spectra of the three catechol based oxidovanadium(IV) complexes in aqueous solutions showed bands at 750 nm (33), 550 nm (28) ( $\text{H}_2\text{O}$ ); 656 nm (69), 540 nm (38) ( $\text{H}_2\text{O}$ ); and 552 nm (9200), 650 nm, sh (8200) ( $\text{CH}_3\text{CN}$ ), respectively. The UV-visible data for  $\text{Na}_2[\text{VO}(\text{rut})(\text{OH})_2] \cdot 5\text{H}_2\text{O}$  (DMSO/ $\text{H}_2\text{O}$ ), 820 nm (42), 660 nm, sh (29), resembles the spectral pattern of the mono-catechol complex. Altogether the experimental measurements in the solid state and in solution point to a M:L 1:1 stoichiometry in the complex.

### 3.3. Antioxidant activity

The radical scavenging power of rutin and  $\text{VORut}$  has been measured against the reactive oxygen species (superoxide,

peroxyl and hydroxyl radicals) and DPPH<sup>•</sup> radical (Fig. S5, ESI<sup>†</sup>).

The flavonoid rutin is not able to cause dismutation of the superoxide radicals. This behavior has been slightly improved by complexation, though its activity is low ( $IC_{50} = 356 \mu\text{M}$ ) (Fig. S5A, ESI<sup>†</sup>). A similar antioxidant improvement has been found for the Znrut complex with respect to rutin.<sup>23</sup> The superoxide radical scavenging power of rutin was reported to be somehow higher, but this effect may be due to the different experimental design.<sup>31</sup> The peroxyl radicals were measured by the thermal decomposition of AAPH following the decay of the spectrometric probe, pyranine. The lag phase (the capacity of a compound to scavenge peroxyl radicals) was calculated based on the consumption time of peroxyl radicals by the compounds, prior to the beginning of pyranine consumption. The scavenging power of rutin against peroxyl radicals (Fig. S5B, ESI<sup>†</sup>) was higher than the effects of the complex and the antioxidant, a vitamin E analog, trolox. The ligand displayed weak antioxidant power against hydroxyl radicals. This behavior has been improved by complexation (Fig. S5C, ESI<sup>†</sup>). Similar results for rutin were previously obtained. Rutin was a better scavenger of DPPH<sup>•</sup> radicals than the complex ( $IC_{50} = 32 \mu\text{M}$  vs.  $44 \mu\text{M}$ , Fig. S5D, ESI<sup>†</sup>). The radical scavenging activity of rutin against DPPH<sup>•</sup> has been reported by several authors. The different data show that  $10 \mu\text{M}$ ,  $30.4 \mu\text{M}$  and  $82 \mu\text{M}$  rutin inhibited 61.7%,<sup>22</sup> 45%,<sup>24</sup> and 90.4%,<sup>31</sup> respectively. Other reports showed that the antioxidant action of the rutin complex of Ni(II) was slightly stronger than that of free rutin<sup>26</sup> with  $IC_{50} = 12.6 \mu\text{M}$  for the complex.<sup>32</sup>

Interestingly, the antioxidant behavior against DPPH<sup>•</sup> was reported for the complex of V(IV)O with rutin<sup>11</sup> and the authors found that there was an improvement of the ligand behavior by complexation and the same trend was reported for the Zn(II) and Ni(II) complexes. In all these complexes the coordination environment (C=O and O<sup>-</sup>) is an acetylacetonate-type one. As it has been mentioned in the Introduction, we found that when

the metal center coordinates to the flavonoid through the carbonyl and one deprotonated adjacent OH group, the resonance established between rings C and/or A allows the stabilization of the flavonoid radical. In these cases, the systems have better antioxidant power. On the contrary, when these groups were not involved in metal coordination, the antioxidant power of the flavonoid has not totally been improved by metal interaction, like in the present case with catechol-type coordination of V(IV)O with rutin.

### 3.4. Human lung cancer cells

**3.4.1. Cell viability assay (MTT method).** The effects of rutin, VO<sub>rut</sub> and the V(IV)O cation were investigated by the conventional MTT assay and the  $IC_{50}$  value for the complex (the concentration that inhibits 50% cell viability) was determined using the SigmaPlot software. Ligand solutions were prepared in DMSO (0.5%)/buffer and DMSO (0.5%) was used as a solvent control, and did not show any significant toxicity. It has been reported that rutin produced a reduction in tumor size (human leukemia HL-60 cells implanted in a murine model), and inhibited the growth of neuroblastoma LAN-5 cells, and colorectal (SW480), cervical (HeLa), breast (MDA-MB231) and ovarian (OVCA433) cancer cell lines, the  $IC_{50}$  values being higher than  $100 \mu\text{M}$ . After 72 h incubation rutin kills cancer cells at relatively high concentrations ( $IC_{50} = 388 \mu\text{M}$ , HT29, and  $710 \mu\text{M}$ , Caco-2 colon cancer cell lines and  $560 \mu\text{M}$ , the A549 human lung cancer cell line).<sup>3</sup> Besides, rutin did not display toxic effects on nontumorigenic HaCaT cells.<sup>33</sup> From our experimental data (Fig. 2A) it can be seen that rutin did not show anticancer activity against the human lung A549 cancer cell line at concentrations up to  $100 \mu\text{M}$ , and that V(IV)O cations inhibited only 16% cell viability. Aqueous solutions of VO<sub>rut</sub> significantly inhibited the growth of lung cancer cells in a dose response manner ( $IC_{50} = 98 \mu\text{M}$ ), improving the anticancer effect of rutin.

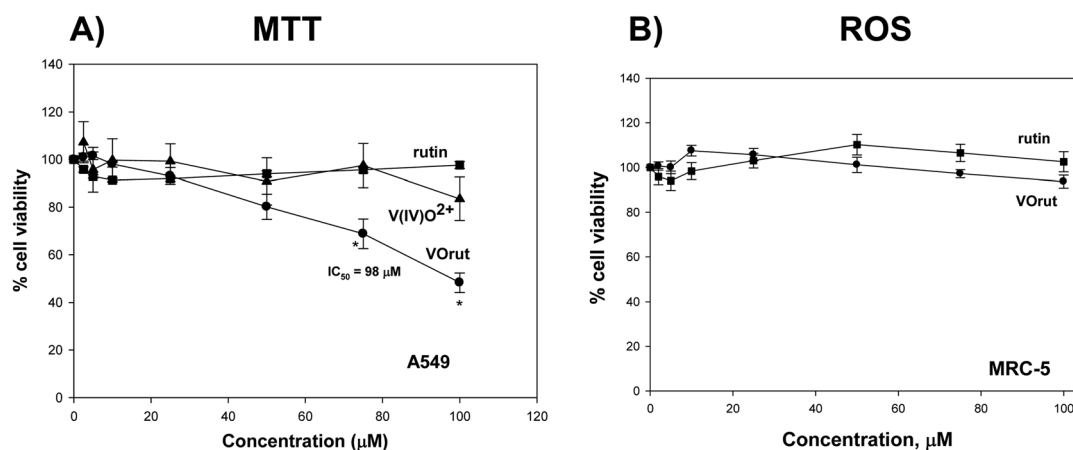


**Fig. 2** Effect of rutin, VO<sub>rut</sub> and oxidovanadium(IV) cations on (A) cancer cell line A549 viability inhibition and (B) effect of rutin and VO<sub>rut</sub> on MRC-5 cell line viability. The cell lines were treated with various concentrations of the compounds for 24 h. The results are expressed as the percentage of the control level and represent the mean  $\pm$  the standard error of the mean (SEM) from three separate experiments. \* significant values in comparison with the control level ( $p < 0.05$ ).

The deleterious effect in cancer cells is selective (Fig. 2B). In the normal human cell culture line of fibroblasts derived from lung tissue, MRC-5, rutin and VOrotin did not inhibit cell viability at the tested concentrations during 24 h (incubation time). In the previous acute study of the VOrot complex with acetylacetonate coordination a  $LC_{50}$  value of  $120 \text{ mg kg}^{-1}$  body weight in fasted balb/c mice has been determined, but these toxic effects were transient.<sup>11</sup>

**3.4.2. Intracellular ROS generation.** It is known that cancer cells have higher levels of ROS than normal cells, and that ROS are responsible for the cancer phenotype.<sup>34</sup> The antioxidant compounds flavonoids can also act as pro-oxidant agents in cancer cells through the interaction of the flavonoid radicals (generated after electron or H donation) with oxygen in the presence of transition metals. Flavonoid radicals therefore generate quinone while molecular oxygen generated superoxide radicals. These radicals are very reactive and can harm essential macromolecules such as proteins or DNA. Flavonoid metal complexes could improve the anti-cancer effects of flavonoids *via* the pro-oxidant behavior that is manifested mainly in cancer cells. To investigate the behavior of rutin and VOrot the levels of intracellular ROS were determined by DCFH-DA assay. This probe is useful for detecting intracellular  $\text{H}_2\text{O}_2$  and oxidative stress. From Fig. 3 it can be seen that VOrot generated intracellular ROS. However, no ROS production in treated cells was determined for both rutin and  $\text{VO(IV)}^{2+}$  cations. Moreover, it has been reported that  $100 \mu\text{M}$  rutin decreased superoxide production by 57% in the A549 cell line, in comparison with untreated cells, using lucigenin chemiluminescence for the detection of superoxide ions.<sup>3</sup>

The increase in the amount of intracellular ROS produced by the complex generated a cancer cell killing effect and hence we assumed that oxidative stress may play a key role in its toxic effect. To confirm this assumption we studied the effect of *N*-acetyl-cysteine (NAC) on the ROS levels (Fig. 3A). The

pretreatment of the cell line with 5 mM NAC and VOrot suppressed the generation of intracellular ROS. The complex elevates the amount of intracellular ROS allowing cancer cells to be selectively killed. When the generation of cellular ROS was suppressed, the cell viability was recovered (Fig. 3B). Then, we can demonstrate the involvement of oxidative stress as one of the mechanisms of lung cancer cell death.

**3.4.3. Cellular glutathione (GSH) depletion.** GSH prevents damage caused by ROS to important cellular components. One of the indices of oxidative stress is the depletion of the non-enzymatic antioxidant glutathione (GSH), producing oxidized glutathione (GSSG) that is toxic to the cell. To support the oxidative stress mechanism of action, the concentrations of GSH and GSSG were measured in A549 cells pretreated with different concentrations of rutin and VOrot and the GSH/GSSG ratio was calculated. As expected, rutin did not alter the GSH and GSSG levels (Fig. 4). The metal complex decreases both GSH and GSH/GSSG, showing that GSH is oxidized to GSSG (decreasing the endogenous antioxidant concentration in the cell and accumulating its oxidation product). The production of cellular ROS, the disruption of one of the natural antioxidant systems (GSH/GSSG) and the absence of toxicity when ROS generation was suppressed allow us to suggest an oxidative stress mediated mechanism of action for the cancer cell killing effect of the complex.

**3.4.4. Morphological changes.** The morphological changes of the A549 cells (5 and  $100 \mu\text{M}$  VOrot incubation, 24 h) are shown in Fig. 5. The toxicity of  $100 \mu\text{M}$  VOrot is determined by the increase of cytoplasm condensation and the presence of pycnotic nuclei. These observations agree with the results obtained in the cell viability studies.

### 3.5. Bovine serum albumin (BSA) interactions

Serum albumin is the most abundant plasma carrier protein in mammals and it is involved in the transport of drugs through

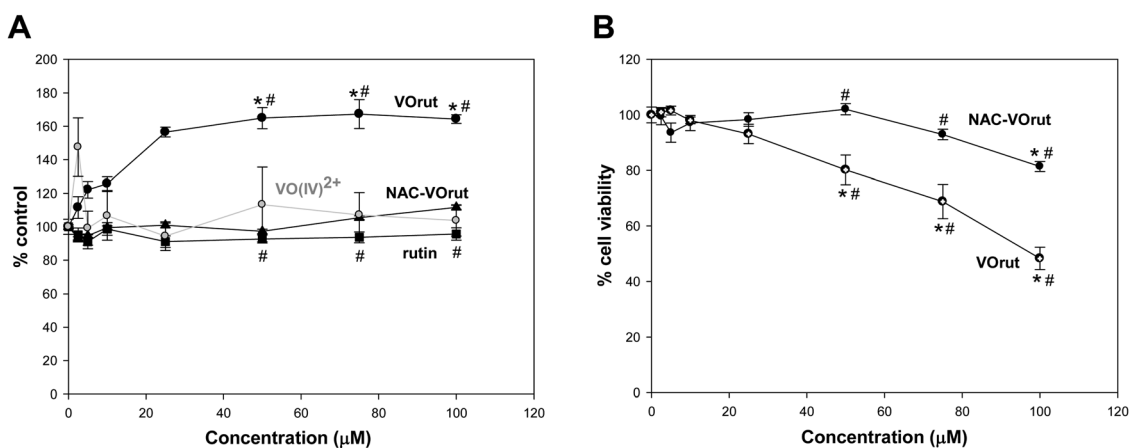


**Fig. 3** (A) Effect of rutin, VOrot and oxidovanadium(IV) cations on H<sub>2</sub>DCFDA oxidation to DCF (A549 cells were incubated at 37 °C in the presence of 10 mM H<sub>2</sub>DCFDA) and the effect of *N*-acetyl-L-cysteine (NAC, 5 mM) on ROS production induced by VOrot. (B) Inhibitory effects of VOrot on A549 cell viability in the presence of *N*-acetyl-L-cysteine (NAC, 5 mM). The cell line was treated with various concentrations of the complex at 37 °C for 24 h. The values are expressed as a percentage of the control level and represent the mean  $\pm$  SEM. \* significant values in comparison with the control level ( $p < 0.05$ ). # significant differences at the same concentration between rutin and VOrot,  $p < 0.05$  (A) and # significant differences at the same concentration between VOrot with NAC and VOrot,  $p < 0.05$  (B).

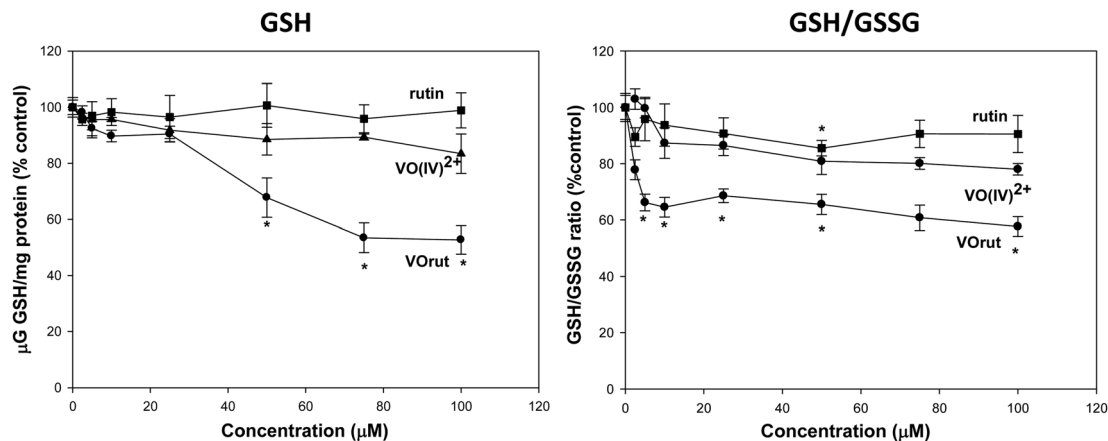


Fig. 4 Effect of rutin, VO(IV)2+ and oxidovanadium(IV) cations on GSH cellular levels and the GSH/GSSG ratio in A549 cells. Results are expressed as the mean  $\pm$  SEM of three independent experiments, \* significant differences in comparison with the control level ( $p < 0.05$ ).

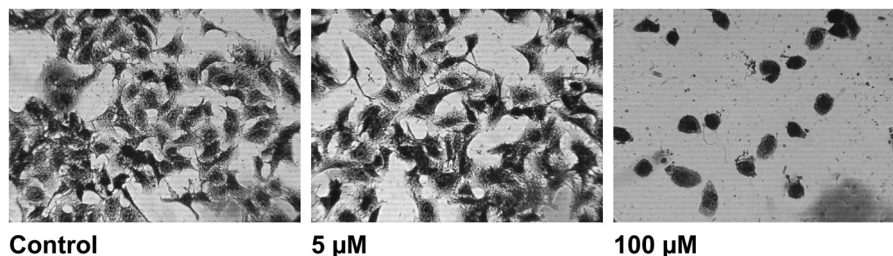


Fig. 5 Effect on the cell morphology of the treatment of the A549 cell line with VO(IV)2+. Cells were incubated for 24 h without the drug (control), and with 5 and 100  $\mu\text{M}$  VO(IV)2+.

the bloodstream. Bovine serum albumin is a serum protein from cows, chemically similar to human serum albumin, but with low cost. Fluorescence quenching measurements have been widely used to study the interactions of compounds with this protein.<sup>35</sup> The intrinsic fluorescence of BSA when excited at 280 nm is due to excitation mainly of the tryptophan residues. The emission spectra of BSA decrease in intensity with an increasing concentration of rutin and its complex (Fig. S6, ESI<sup>†</sup>).

To determine the quenching constants the fluorescence data have been analyzed with the Stern–Volmer equation at different temperatures:<sup>35</sup>

$$F_0/F = 1 + K_q\tau_0[Q] = 1 + K_{sv}[Q] \quad (1)$$

where  $F_0$  and  $F$  are the fluorescence intensities in the absence and presence of the quencher, respectively;  $K_q$  is the bimolecular quenching constant;  $\tau_0$  is the lifetime of the fluorophore in the absence of the quencher;  $[Q]$  is the concentration of the quencher and  $K_{sv}$  is the Stern–Volmer quenching constant, which can be obtained from the slope of eqn (1). The Stern–Volmer plots are shown in Fig. S7 (ESI<sup>†</sup>).

The average values of  $K_{sv}$  were obtained from the slopes of the straight lines by linear regression treatment (Table 1). The quenching constants were calculated considering a fluorescence lifetime  $\tau_0$  of BSA of  $1.0 \times 10^{-8}$  s. Taking into account that the scattering collision (dynamic) quenching of various

Table 1 Stern–Volmer constant ( $K_{sv}$ ), quenching rate constant ( $K_q$ ), binding constant ( $K_a$ ) and  $n$  binding sites for the interaction of rutin and VO(IV)2+ with BSA (6  $\mu\text{M}$ ) in Tris–HCl buffer (0.1 M, pH 7.4)

	$T$ (K)	$K_{sv}$ ( $10^4$ ) ( $\text{M}^{-1}$ )	$K_q$ ( $10^{12}$ ) ( $\text{M}^{-1} \text{s}^{-1}$ )	$K_a$ ( $10^4$ ) ( $\text{M}^{-1}$ )	$n$
Rutin	298	$5.99 \pm 0.21$	$5.99 \pm 0.21$	$19.8 \pm 0.52$	$1.13 \pm 0.11$
	303	$4.95 \pm 0.21$	$4.95 \pm 0.21$	$10.2 \pm 0.45$	$1.08 \pm 0.10$
	310	$4.85 \pm 0.15$	$4.85 \pm 0.15$	$9.75 \pm 0.20$	$1.07 \pm 0.04$
VO(IV)2+	298	$6.66 \pm 0.24$	$6.66 \pm 0.24$	$60.4 \pm 0.21$	$1.22 \pm 0.05$
	303	$6.28 \pm 0.41$	$6.28 \pm 0.41$	$52.1 \pm 0.51$	$1.21 \pm 0.12$
	310	$6.17 \pm 0.24$	$6.17 \pm 0.24$	$43.1 \pm 0.24$	$1.18 \pm 0.06$

quenchers with biopolymers is  $2.0 \times 10^{10} \text{ L mol}^{-1} \text{ s}^{-1}$ , the high  $K_q$  values obtained in this study indicated static quenching between BSA and the compounds due to their binding and complex formation between the protein and quencher.<sup>35</sup>

For static quenching, from the plot of  $\log[(F_0 - F)/F]$  vs.  $\log[Q]$ , the binding constants  $K_a$  and the number of binding sites  $n$  were determined (Fig. S8, ESI<sup>†</sup> and Table 1), according to the following equation:

$$\log[(F_0 - F)/F] = \log K_a + n \log[Q] \quad (2)$$

Only one binding site for the bonding between BSA and the compounds was determined. The stability constants decreased

with temperature according to a decrease in stability of the BSA-compound binding.

The value of  $K_a$  will directly correlate with the transport, disposition, and *in vivo* efficacy of a compound. The magnitude of our experimental values (*ca.*  $10^5 \text{ M}^{-1}$ ) suggested moderate affinity of the compounds for BSA and that they could be stored and removed by BSA. Moreover, and despite the different procedures used, our data for  $K_{SV}$  and  $K_a$  for rutin were similar to those previously reported. Total quenching using tryptophan fluorescence was reported for rutin-BSA at a molar ratio of 25/1 ( $K_{SV} = 19.2 \times 10^4 \text{ M}^{-1}$ ), the binding affinity being lower than for its aglycon, quercetin. The rutinose disaccharide makes rutin less hydrophobic and more bulky, producing steric hindrance for the hydrophobic pocket of Trp 212.<sup>36</sup> Moreover, a static quenching process through the Trp 212 residue was reported for the interaction rutin-BSA ( $K_{SV} = 3.2 \times 10^4 \text{ M}^{-1}$ ,  $K_a = 4.40 \times 10^5 \text{ M}^{-1}$ , binding sites = 1.40).<sup>37</sup> The complex interacted more strongly with BSA than rutin. The interaction of rutin and the V(IV)O complexes (acetylacetonate like coordination) with BSA has previously been reported<sup>10</sup> and the increased fluorescence intensities produced by the complexes were ascribed to a higher rigidity of the ligand in the complex.

Basically, four main types of forces may be involved in protein-compound interactions: hydrogen bonds and electrostatic, van der Waals or hydrophobic forces, and they were evaluated through the thermodynamic parameters (the van't Hoff equation, eqn (3)):

$$\ln K_a = -\Delta H/RT + \Delta S/R \quad (3)$$

where  $K_a$  is analogous to the associative binding constants at the corresponding experimental temperature  $T$  and  $R$  is the gas constant. The free energy change ( $\Delta G$ ) can be estimated from the following relationship (4):

$$\Delta G = \Delta H - T\Delta S \quad (4)$$

The thermodynamic parameters are summarized in Table 2.

The negative sign for the free energy ( $\Delta G$ ) shows that the binding processes are spontaneous. The negative value of  $\Delta H$  for both compounds suggested that the binding to BSA is an exothermic process and then the association constant decreases with increasing temperature. A negative value of  $\Delta S$  suggests that the binding process is predominately enthalpy driven by means of hydrogen bonding and van der Waals force interactions while a positive  $\Delta S$  change occurs when the water molecules are arranged around the ligand and the protein acquires a more random configuration as a result of hydrophobic interactions.

**Table 2** Thermodynamic parameters for the interactions between rutin and VOrut and BSA

	$\Delta H$ (kJ mol <sup>-1</sup> )	$\Delta S$ (J mol <sup>-1</sup> )	$\Delta G$ (kJ mol <sup>-1</sup> )
Rutin	-42.6	-42.7	-29.9 (298 K) -29.7 (303 K) -29.4 (310 K)
VOrut	-21.6	38.2	-33.0 (298 K) -33.2 (303 K) -33.4 (310 K)

From Table 2 it can be seen that van der Waals forces and hydrogen bonding play a significant role in the binding of rutin to BSA. The negative enthalpy ( $\Delta H$ ) and positive entropy ( $\Delta S$ ) values of the interaction of VOrut and BSA indicate that specific electrostatic interactions played a major role.<sup>38</sup> Taking into account the resonant structures of rutin and tryptophan and tyrosine, it is reasonable to expect  $\pi$ - $\pi$  interactions between the aromatic rings of BSA and the compounds. On the other hand, the anionic nature of the complex  $[\text{VO}(\text{rutin})(\text{OH})_2]^{2-}$  allows electrostatic interactions with BSA, and stronger binding constants for the BSA-VOrut system.

## 4. Discussion

Two solid complexes formed between the oxidovanadium(IV) cation and rutin have previously been synthesized and characterized as  $[\text{VO}(\text{rutin})(\text{H}_2\text{O})_2]_2(\text{SO}_4) \cdot 4\text{H}_2\text{O}$  and  $[\text{VO}(\text{Rut})_2] \cdot 4\text{H}_2\text{O}$ .<sup>10,11</sup> In these complexes an acetylacetonate-type coordination sphere around the metal center was found. Attempts to obtain the same complexes gave the solid  $\text{Na}_2[\text{VO}(\text{rut})(\text{OH})_2] \cdot 5\text{H}_2\text{O}$  complex (see Fig. 6). Elemental analysis, thermogravimetric determinations and FTIR and EPR spectroscopies allow the characterization of the solid compound.

The complex displayed catechol-like coordination in which deprotonated oxygen atoms in 3'- and 4'-positions are bonded to the metal center. The VOrut complex improved the antioxidant potency of the ligand only against superoxide and hydroxyl radicals but not against peroxy and DPPH• radicals. This behavior is consistent with our previous findings: the better antioxidant VOflavonoid complexes are those in which the carbonyl group is involved in the metal interaction, bearing maltol- or acetylacetonate-type coordination. At this point it should be noted that the antioxidant effect of the  $[\text{VO}(\text{rut})_2] \cdot 4\text{H}_2\text{O}$  complex in which the C=O and deprotonated 5-OH groups are involved in metal coordination was reported to have greater antioxidant power against DPPH• than the ligand, because of the generated electronic delocalization that stabilized the phenoxyl radical that resulted from the interaction with free radicals.

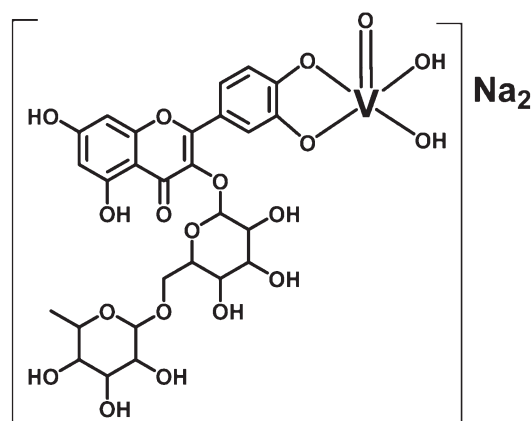


**Fig. 6** Schematic representation of  $\text{Na}_2[\text{VO}(\text{rut})(\text{OH})_2] \cdot 5\text{H}_2\text{O}$ .

**Table 3** Cell viability and cellular ROS generation for 100  $\mu\text{M}$  concentrations of the different compounds incubated for 24 h in the A549 cancer cell line. Basal: 100%

	Apigenin <sup>17</sup>	ApigeninVO <sup>17</sup>	Luteolin <sup>7</sup>	LuteolinVO <sup>7</sup>	Diosmin <sup>8</sup>	DiosminVO <sup>8</sup>	Baicalin <sup>11</sup>	BaicalinVO <sup>11</sup>	V(IV)O <sup>10</sup>	Rutin	RutinVO
ROS (%)	150	150	200	263	140	200	150	266	100	100	170
Cell viability (%)	81	75	50	50	104	69	78	64	84	98	48

Furthermore, the biological properties of different complexes of V(IV)O and flavonoids are highly dependent on the substituents of the flavonoids. It is known that during the transition from normal tissue to carcinoma, cells produce high levels of ROS due to their metabolic aberrations, and because cancer cells are more vulnerable to ROS than normal cells, ROS generating compounds can kill cancer cells selectively. We have previously determined in the human lung cancer A549 cell line that some complexes with glycosylated flavonoids produced a higher improvement in the generation of cellular ROS with respect to the ligands and then the cells were more vulnerable to damage by those ROS insults (Table 3).

As can be seen from Table 3, complexation of the non-glycosylated flavonoids apigenin and luteolin did not improve the anticancer effects of the flavonoids.<sup>7,17</sup> However, when baicalin and diosmin coordinated to the oxidovanadium(IV) cation the production of cellular ROS is increased 1.8 and 1.4 times, respectively.<sup>8,9</sup> The anticancer effects of both complexes associated with this oxidative stress are increased 1.2 times for BaicalinVO and 1.5 times for DiosminVO.

To confirm these findings and determine a structure–activity relationship for the anticancer effects of these complexes, we have selected herein the glycosylated flavonoid rutin. The complex displayed the ability to generate ROS and deplete cellular antioxidants: cellular ROS increased 1.7 times upon complexation and the anticancer effect of VORut was 2 times higher than the effect of the glycosylated flavonoid rutin. Then, a relationship between the structure of the VOflavonid complexes and their activities could be determined: the V(IV)O complexes of glycosylated flavonoids show a better improvement of the anticancer action. These findings were also discussed for glycosidic antibiotics such as daunomycin and adriamycin in which the glycosidic residues are crucial to their activity. The role of the glycosidic residue in the biological activity of glycosidic antibiotics has been explained by the intercalation of the aglycone with DNA, the aminosugar being the anchoring unit which fills the minor groove, displacing water and ions from the groove. Hence, the aminosugar may interact with polymerases, preventing or retarding the action of these enzymes.<sup>39</sup> Therefore, and in addition to ROS production, the higher rigidity of the ligand rutin in the complex, previously described by the increased fluorescence intensities for the complexes,<sup>10</sup> may generate better intercalation of the complexed ligand with DNA, the sugar being the anchoring unit which fills the minor groove and is able to interact with polymerases.

The binding constants obtained for the ligand and the complex with BSA are in the suitable range of binding by which the carrier can be useful for the transportation of both compounds and also their release into solution and cells.

## 5. Conclusion

In summary, we present more evidence that the oxidovanadium(IV) complexes with glycosylated flavonoids improved the anticancer action of the ligand in lung cancer A549 cell lines. The complex VORut bearing catechol-like coordination displayed stronger anticancer activity and cellular ROS generation than rutin. It inhibited cellular growth, and led to a substantial increase in ROS formation and to a decrease of the GSH/GSSG ratio. Furthermore, upon addition of NAC the anticancer effect has been reverted. These results evidenced that the complex induce cell death *via* an oxidative stress mechanism, acting as a pro-oxidant agent in cancer cells despite its antioxidant behavior displayed in the *in vitro* experiments without cells. The complex can also be transported and delivered by BSA.

## Abbreviations

AAPH	2,2-Azobis (2-amidinopropane)dihydrochloride
ABTS	2,2'-Azino-bis(3-ethyl-benzothiazoline-6-sulfonic acid diammonium salt)
DMEM	Dulbecco's modified Eagle medium
DPPH	2,2-Diphenyl-1-picrylhydrazyl radical
EDTA	Ethylenediaminetetraacetic acid
H <sub>2</sub> DCFDA	2',7'-Dichlorodihydrofluorescein diacetate
MTT	3-(4,5-Dimethylthiazol-2-yl)-2,5-diphenyltetrazolium bromide
NAC	N-Acetylcysteine
NADH	Nicotinamide adenine dinucleotide
NBT	Nitroblue tetrazolium
PBS	Phosphate buffered saline
PMS	Phenazine methosulfate
ROS	Reactive oxygen species
SOD	Superoxide dismutase
Tris-HCl	Tris(hydroxymethyl)aminomethane-HCl
Trolox	6-Hydroxy-2,5,7,8-tetramethylchroman-2-carboxylic acid

## Conflicts of interest

There are no conflicts to declare.

## Acknowledgements

This work was supported by UNLP (X/736), CONICET PIP (0611-0550), UNL (CAI + D 2016-50420150100070LI), CICPBA, and ANPCyT (PICT 2016-1814, 2017-2186), Argentina. EGF and LGN are research fellows of CONICET. PAMW is a research fellow of

1 CICPBA, Argentina. HG and VRM are fellowship holders from CONICET.

## References

- 1 C. J. Dufresne and E. R. Farnworth, *J. Nutr. Biochem.*, 2001, **12**, 404–421.
- 2 A. Ganeshpurkar and A. K. Saluja, *Saudi Pharm. J.*, 2017, **25**, 149–164.
- 3 M. ben Sghaier, A. Pagano, M. Mousslim, Y. Ammari, H. Kovacic and J. Luis, *Biomed. Pharmacother.*, 2016, **84**, 1972–1978.
- 4 R. F. V. De Souza and W. F. De Giovani, *Redox Rep.*, 2004, **9**, 97–104.
- 5 M. Samsonowicz, E. Regulska and M. Kalinowska, *Chem.-Biol. Interact.*, 2017, **273**, 245–256.
- 6 A. Goc, *Cent. Eur. J. Biol.*, 2006, **1**, 314–332.
- 7 L. G. Naso, L. Lezama, M. Valcarcel, C. Salado, P. Villacé, D. Kortazar, E. G. Ferrer and P. A. M. Williams, *J. Inorg. Biochem.*, 2016, **157**, 80–93.
- 8 L. G. Naso, V. R. Martínez, L. Lezama, C. Salado, M. Valcarcel, E. G. Ferrer and P. A. M. Williams, *Bioorg. Med. Chem.*, 2016, **24**, 4108–4119.
- 9 J. J. Martínez Medina, L. G. Naso, A. L. Pérez, A. Rizzi, E. G. Ferrer and P. A. M. Williams, *J. Inorg. Biochem.*, 2017, **166**, 150–161.
- 10 V. Uivarosi, S. F. Barbuceanu, V. Aldea, C. C. Arama, M. Badea, R. Olar and D. Marinescu, *Molecules*, 2010, **15**, 1578–1589.
- 11 S. Roy, S. Majumdar, A. Kumar Singh, B. Ghosh, N. Ghosh, S. Manna, T. Chakraborty and S. Mallick, *Biol. Trace Elem. Res.*, 2015, **166**, 183–200.
- 12 D. Sanna, V. Ugone, G. Lubinu, G. Micera and E. Garribba, *J. Inorg. Biochem.*, 2014, **140**, 173–184.
- 13 H. Onishi, *Photometric determination of traces of metals*, Wiley, New York, 4th edn, 1988.
- 14 S. Stoll and A. Schweiger, *J. Magn. Reson.*, 2006, **178**, 42–55.
- 15 I. Ali, W. A. Wani and K. Saleem, *Synth. React. Inorg., Met.-Org., Nano-Met. Chem.*, 2013, **43**, 1162–1170.
- 16 I. P. Bulatov and M. I. Kalinkin, *Practical Manual of Photometric Analysis Chemistry*, Leningrad, 5th edn, 1986.
- 17 J. J. Martínez Medina, L. G. Naso, A. L. Pérez, A. Rizzi, N. B. Okulik, E. G. Ferrer and P. A. M. Williams, *J. Photochem. Photobiol., A*, 2017, **344**, 84–100.
- 18 J. Van Meerloo, G. J. L. Kaspers and J. Cloos, *Methods Mol. Biol.*, 2011, **731**, 237–245.
- 19 M. Bradford, *Anal. Biochem.*, 1976, **254**, 248–254.
- 20 L. U. Ling, K. B. Tan, H. Lin and G. N. C. Chiu, *Cell Death Dis.*, 2011, **2**, e129–e140.
- 21 P. J. Hissin and R. Hilf, *Anal. Biochem.*, 1976, **74**, 214–226.
- 22 M. Samsonowicz, I. Kaminska, M. Kalinowska and W. Lewandowski, *Spectrochim. Acta, Part A*, 2015, **151**, 926–938.
- 23 N. E. Andrades Ikeda, E. M. Novak, D. A. Maria, A. Segin Velosa and R. M. Silva Pereira, *Chem. – Biol. Interact.*, 2015, **239**, 184–191.
- 24 N. D. Chasteen, Vanadyl(IV) spin probes, inorganic and biochemical aspects, in *Biological Magnetic Resonance*, ed. L. J. Berliner and J. Reuben, Plenum, New York, 1981, vol. 3.
- 25 C. R. Cornman, E. P. Zovinka, Y. D. Boyajian, K. M. Geiser-Bush, P. D. Boyle and P. Singh, *Inorg. Chem.*, 1995, **34**, 4213–4219.
- 26 A. Raza, S. Bano, X. Xu, R. X. Zhang, H. Khalid, F. M. Iqbal, C. Xia, J. Tang and Z. Ouyang, *Biol. Trace Elem. Res.*, 2017, **178**, 160–169.
- 27 N. P. Slabbert, *Tetrahedron*, 1977, **33**, 821–824.
- 28 M. J. Sever and J. J. Wilker, *Dalton Trans.*, 2004, 1061–1072.
- 29 S. R. Cooper, Y. B. Koh and K. N. Raymond, *J. Am. Chem. Soc.*, 1982, **104**, 5092–5102.
- 30 D. Sanna, G. Sciortino, V. Ugone, G. Micera and E. Garribba, *Inorg. Chem.*, 2016, **55**, 7373–7387.
- 31 J. Yang, J. Guo and J. Yuan, *LWT-Food Sci. Technol.*, 2008, **41**, 1060–1066.
- 32 S. A. Cherrak, N. Mokhtari-Soulimane, F. Berroukeche, B. Bensenane, A. Cherbonnel, H. Merzouk and E. Mourad, *PLoS One*, 2016, **11**, e0165575, DOI: 10.1371/journal.pone.0165575.
- 33 A. J. Alonso-Castro, F. Domínguez and A. García-Carrancá, *Arch. Med. Res.*, 2013, **44**, e346–e351.
- 34 L. Gibellini, M. Pinti, M. Nasi, S. De Biasi, E. Roat, L. Bertocelli and A. Cossarizza, *Cancers*, 2010, **2**, 1288–1311, DOI: 10.3390/cancers2021288.
- 35 *Principles of Fluorescence Spectroscopy*, ed. J. R. Lakowicz, Springer Science & Business Media, New York, 2013.
- 36 A. Papadopoulou, R. Green and R. Frazier, *J. Agric. Food Chem.*, 2005, **53**, 158–163.
- 37 M. A. Jhonsi, S. Selvaraj, G. Paramaguru, P. Venuvanalingam and R. Renganathan, *Z. Phys. Chem.*, 2011, **225**, 441–454.
- 38 P. A. Ross and S. Subramunian, *Biochemistry*, 1981, **20**, 3096–3102.
- 39 V. Křen and T. Řezanka, *FEMS Microbiol. Rev.*, 2008, **32**, 858–889.